Immunity
Article

Prolonged Interleukin-2Rα Expression on Virus-Specific CD8$^+$ T Cells Favors Terminal-Effector Differentiation In Vivo

Vandana Kalia,[1,5] Surojit Sarkar,[1,5] Shruti Subramaniam,[2] W. Nicholas Haining,[3] Kendall A. Smith,[4] and Rafi Ahmed[1,*]
[1]Emory Vaccine Center, Emory University School of Medicine, Atlanta, GA 30322, USA
[2]Loma Linda University, Loma Linda, CA 92350, USA
[3]Pediatric Oncology, Dana-Farber Cancer Institute, Pediatric Hematology and Oncology, Children's Hospital, Boston, Harvard School of Medicine, MA 02115, USA
[4]Cornell University, New York, NY 14853, USA
[5]These authors contributed equally to this work
*Correspondence: rahmed@emory.edu
DOI 10.1016/j.immuni.2009.11.010

SUMMARY

CD25, the high-affinity interleukin-2 (IL-2) receptor α chain, is rapidly upregulated by antigen-specific CD8$^+$ T cells after T cell receptor stimulation. Here, we demonstrate that during an acute viral infection, CD25 expression is quite dynamic—after initial upregulation, a subset of virus-specific T cells sustains CD25 expression longer than the rest. At this time when there is distinct heterogeneity in CD25 expression, examination of the in vivo fate of effector cells revealed that CD25^{lo} cells, which are relatively less sensitive to IL-2, preferentially upregulate CD127 and CD62L and give rise to functional long-lived memory cells. In contrast, CD25^{hi} cells perceiving prolonged IL-2 signals proliferate more rapidly, are prone to apoptosis, exhibit a more pronounced effector phenotype, and appear to be terminally differentiated. Consistent with this, sustained IL-2 receptor signaling during expansion drove terminal-effector differentiation. These data support the hypothesis that prolonged IL-2 signals during priming promote terminal-effector differentiation.

INTRODUCTION

After antigen encounter, naive CD8$^+$ T cells undergo extensive proliferation and differentiate into effector cells. Several studies now confirm that an initial encounter with antigen launches CD8$^+$ T cells into a "program" of proliferation and effector differentiation (Kaech and Ahmed, 2001; Kalia et al., 2006; Mercado et al., 2000; van Stipdonk et al., 2003; van Stipdonk et al., 2001; Williams and Bevan, 2007). Moreover, the onset and kinetics of contraction and memory CD8$^+$ T cell fate are also programmed (Badovinac et al., 2002; Kaech and Ahmed, 2001). Programming implies that quality, quantity, and context of the initial signal impact CD8$^+$ T cell fate. However, defining the precise signals that promote differentiation of effector and memory CD8$^+$ T cells has been challenging, due to a lack of molecular markers that effectively distinguish memory fated cells (memory precursors [MP]) from end-stage effectors (terminal effectors [TEs]). An increased impetus in this area in recent years has led to the delineation of several markers (IL-7Rα, CD62L, IL-2, and KLRG-1) (Joshi et al., 2007; Kaech et al., 2003; Marzo et al., 2005; Sarkar et al., 2008; Wherry et al., 2003) that can effectively distinguish MP from TE cells. The presence of KLRG-1^{int} memory fated cells in the pool of expanding CD8$^+$ T cells suggests that signals that promote memory differentiation are received during the priming phase of the immune response and allows one to explore the signals and mechanisms regulating the generation of these subsets.

Various signals, including the strength and duration of infection and T cell receptor (TCR) stimulation, activation status and type of antigen-presenting cells, costimulation, CD4$^+$ T cell help, inflammatory cytokines, and growth factors are implicated in regulating T cell fate decisions (Ahmed and Rouse, 2006; Kalia et al., 2006; Williams and Bevan, 2007). Curtailing the duration of antigen promotes the differentiation of long-lived lymphoid memory cells (Sarkar et al., 2008). However, TCR signals are not solely responsible for the diverse fates of responding T cells. Among various environmental cues, the role of IL-2 in impacting T cell responses has been extensively investigated (Gillis et al., 1978; Lenardo, 1991; Malek, 2008; Pandiyan et al., 2007; Smith, 1988). Although originally defined as a positive growth factor for T cells, IL-2 can exert both positive and negative effects (Cousens et al., 1995; Sadlack et al., 1993; Suzuki et al., 1995). Previous studies involving *Il2*$^{-/-}$ or *Il2rα*$^{-/-}$ mice were complicated by development of autoimmunity, but a recent study employed a mixed chimera strategy, in which T cells lacking the high-affinity IL-2Rα were followed in a wild-type environment (Williams et al., 2006). Although the number of developing effector and memory cells was not affected by the lack of IL-2Rα, secondary responses of CD8$^+$ T cells were compromised, thus leading to the conclusion that IL-2 signals are important in programming memory cells with robust recall responses. With the goal of evaluating the requirement of IL-2 during different stages of CD8$^+$ T cell differentiation, other studies employed the strategy of in vivo IL-2 administration (Blattman et al., 2003; Cheng and Greenberg, 2002; Cheng et al., 2002). This approach demonstrated that excessive IL-2 signals during

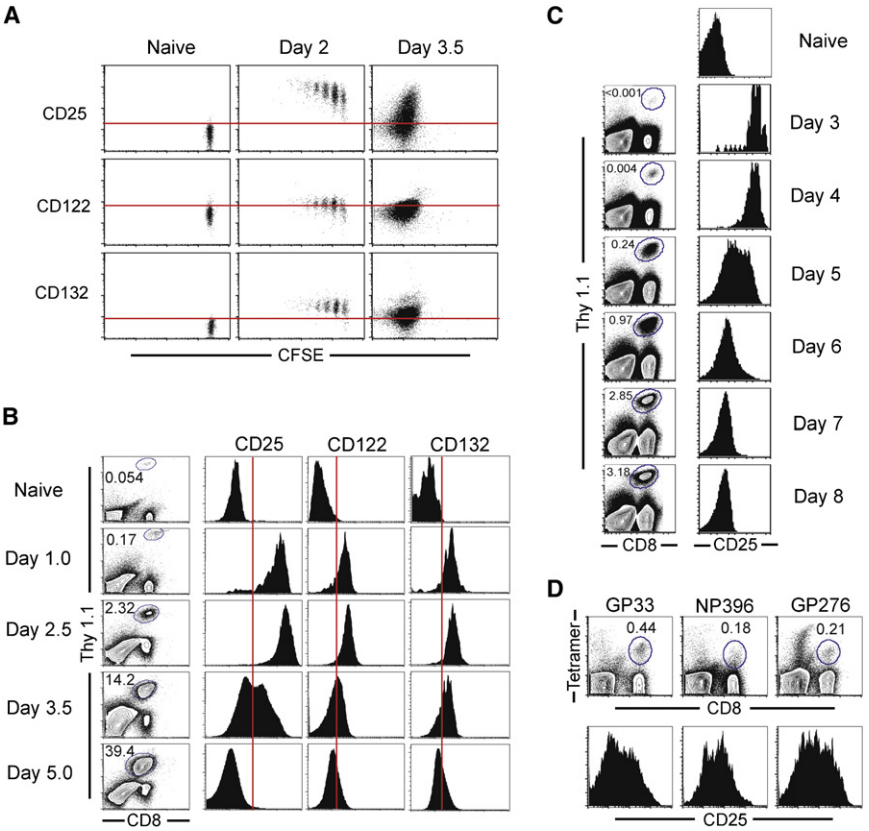

Figure 1. Kinetics of IL-2Rα, β, and γ Chain Expression

(A) Approximately 1 × 10^6 CFSE-labeled transgenic P14 CD8$^+$ T cells, specific for the D^bGP33 epitope, were adoptively transferred into C57Bl/6 mice. At days 2 and 3.5 after infection, antigen-specific CD8$^+$ Thy1.1$^+$ cells were analyzed for CD25, CD122, and CD132 expression with respect to cell division as depicted by CFSE dilution. Uninfected mice were used as naive controls. Red lines depict the expression of indicated markers in naive CD8$^+$ T cells. Dot plots are representative of five independent experiments with two to three replicates.

(B) Chimeric B6 mice containing 1 × 10^6 transgenic P14 CD8$^+$ T cells were infected with LCMV. Splenocytes were isolated at days 1, 2.5, 3.5, and 5 after LCMV infection and P14 cells were analyzed for CD25, CD122, and CD132 expression by direct ex vivo staining of splenocytes. Red lines mark the expression of CD25, CD122, and CD132 in naive cells. Representative data from five independent experiments with two to three replicates are presented.

(C) P14 chimeric mice adoptively transferred with 1 × 10^3 P14 transgenic cells were infected with LCMV. CD8$^+$ Thy1.1$^+$ splenocytes were analyzed for CD25 expression at days 3–8 after infection. Representative histogram plots from two independent experiments with three replicates are presented.

(D) Wild-type B6 mice were infected with LCMV and splenocytes were analyzed for CD25 expression at day 5 after infection after gating CD8$^+$ GP33$^+$, CD8$^+$NP396$^+$, or CD8$^+$GP276$^+$ cells. Presented data are representative of two independent experiments with three replicates.

priming and expansion resulted in increased contraction, whereas IL-2 administration during contraction led to enhanced cell survival. Although, both approaches demonstrated a role of IL-2 in modulating CD8$^+$ T cell responses, the precise effect of IL-2 (positive or negative) on memory and the timing of IL-2 action remain to be clearly defined.

In this study, we have examined the role of IL-2 signals in CD8$^+$ T cell differentiation by using the mouse model of acute infection with lymphocytic choriomeningitis virus (LCMV). Our results show that IL-2 plays a major role in CD8$^+$ T cell programming and that prolonged IL-2 signals promote terminal-effector differentiation in vivo.

RESULTS

Dynamic Expression of IL-2R α, β, and γ Chains during CD8$^+$ T Cell Priming

To better understand the role of IL-2 signals in programming CD8$^+$ T cell responses, we performed a longitudinal analysis of the expression of IL-2 receptor on virus-specific cells after an acute LCMV infection. The high-affinity IL-2R is a heterotrimer of CD25, the high-affinity IL-2Rα chain, the IL-2Rβ (CD122), and the common γ-chains (CD132) (Malek, 2008). CD25 imparts high-affinity binding to IL-2, whereas the β- and the γ-chains serve to efficiently transduce IL-2 signals via signaling motifs in their cytoplasmic tails. CD25 expression was uniformly induced on antigen-specific CD8$^+$ T cells early after infection (days 1–2). Additionally, CD25 induction increased with increasing rounds of cell division, as delineated by CFSE dilution (Figure 1A). Approximately day 3.5 after infection, a subset of antigen-specific T cells selectively downregulated their expression of CD25, such that two distinct populations of CD25^{lo} and CD25^{hi} cells were discernable (Figures 1A and 1B). Subsequently, at day 5 after infection, when antigen is largely cleared from the system, all antigen-specific CD8$^+$ T cells downregulated CD25 expression (Figure 1B). Similar to the IL-2Rα chain, the β- and γ-chains were also upregulated after TCR stimulation in a cell division-dependent manner (Figure 1A). After antigen clearance, CD122 and CD132 expression decreased slightly, but was maintained at higher than naive amounts and no heterogeneity in CD122 and CD132 expression was found, as was the case with CD25. It is noteworthy that the heterogeneity in CD25 expression was observed not only with higher precursor frequencies of transgenic CD8$^+$ T cells (Figures 1A and 1B) but was also seen at lower precursor frequencies (10^2 antigen-specific cells), as well as in endogenous GP33, NP396, and GP276 tetramer-specific cells in B6 mice (Figures 1C and 1D). This observed heterogeneity in CD25 expression is suggestive of IL-2 playing a role in differential programming of CD8$^+$ T cells.

Differential CD25 Expression Is Associated with Differences in IL-2 Signal Transduction

CD25 expression is rapidly upregulated by TCR signals, and is maintained by a positive feedback loop via enhanced IL-2 signals (Malek, 2008). To understand if IL-2 may be regulating the heterogeneity in CD25 expression, we measured the amount of IL-2 in spleens of mice infected with LCMV at different days after infection. This analysis was done in B6 mice, and also in mice that received P14 transgenic CD8+ T cells. In both cases, peak of CD25 expression followed the peak of splenic IL-2 production (Figures 1A, 1B, and 2A and Figure S1 available online). Manifestation of CD25 heterogeneity correlated with a substantial drop in splenic IL-2 concentrations; in the case of P14 chimeric mice, CD25 heterogeneity was evident at day 3.5 and IL-2 concentrations dropped down to near basal amounts at this time point (Figures 1A, 1B, and 2A). Similarly, in the case of B6 mice, CD25 heterogeneity at day 5 correlated with decreased IL-2 amounts at day 5 in the spleen (Figures 1C, 1D, and 2A). These data provide correlative evidence that CD25 heterogeneity may result from differential IL-2 signals under conditions of limiting IL-2. When we blocked IL-2 signals from days 0–3.5 postinfection, we found a decrease in the CD25 expression compared to untreated controls (Figure 2B). Thus, IL-2 signals appear to be important in regulating CD25 expression and heterogeneity.

To determine whether higher CD25 expression correlated with increased IL-2 signaling, we tested the ability of $CD25^{hi}$ and $CD25^{lo}$ cells to induce phosphorylation of STAT-5 after in vitro or in vivo IL-2 stimulation. In both cases of in vitro (Figure 2C) and in vivo (Figure 2D) stimulation, we found that $CD25^{hi}$ cells transduced IL-2 signals more efficiently than $CD25^{lo}$ cells, such that ~2-fold greater STAT5 phosphorylation (fold-over unstimulated) was observed in $CD25^{hi}$ cells (Figures 2C and 2D). These results demonstrate that activated $CD8^+$ T cells that express relatively more cell surface CD25 are more efficient at perceiving and transducing IL-2 signals.

CD25 Heterogeneity Is Associated with Differential Expression of Effector Molecules

To investigate whether the $CD25^{lo}$ and $CD25^{hi}$ virus-specific $CD8^+$ T cells discernable at 3.5 days after infection may have assimilated differential signals, we next evaluated their phenotypic and functional properties (Figure 3). Both subsets were activated as demonstrated by similar CD44 upregulation relative to naive cells. Both subsets also downregulated CD127 and CD62L, and upregulated KLRG-1 expression similarly (Figure 3A). We observed that at the mRNA level, $CD25^{hi}$ cells exhibited more pronounced downregulation of CD62L, CD127, and CCR7 (Figure 3B and 3C), suggesting enhanced effector differentiation. Consistent with this possibility, $CD25^{hi}$ cells expressed modestly higher amounts (1.4-fold) of intracellular granzyme B (Figures 3B and 3C). Moreover, mRNA of granzymes (Figure 3B) and perforin (Figure 3C) were also higher in $CD25^{hi}$ cells. Despite modestly lower expression of effector genes in $CD25^{lo}$ cells, both subsets exhibited largely similar direct ex vivo killing activity (Figure 3D), demonstrating that both $CD25^{hi}$ and $CD25^{lo}$ cells had differentiated into equally potent killer cells. T-bet is an important regulator of effector differentiation, and increased T-bet expression correlates with terminal-effector differentiation during later stages of the immune response (Figure S2). Consistent with their effector differentiation status, $CD25^{hi}$ and $CD25^{lo}$ subsets had similarly upregulated T-bet expression by ~50-fold compared to naive cells (Figures 3B and 3C). The production of effector cytokines, IFN-γ and TNF-α after in vitro peptide stimulation, was also largely similar in both subsets (Figure 3E), although IFN-γ mRNA expression was slightly elevated in $CD25^{hi}$ cells (Figure 3B). IL-2 production is typically associated with naive and central memory cells and is progressively lost in $CD8^+$ T cells with advanced effector differentiation (Badovinac and Harty, 2006; Sarkar et al., 2008; Intlekofer et al., 2007; Wherry et al., 2003). Consistent with this, we observed that $CD25^{hi}$ cells produced substantially lower amounts of IL-2 compared to the $CD25^{lo}$ cells (Figure 3E). Lower IL-2 production by $CD25^{hi}$ cells also correlated with increased expression of *Blimp-1* mRNA (Figures 3B and 3C), which is a negative regulator of IL-2. Thus, collectively, these data demonstrate that both $CD25^{lo}$ and $CD25^{hi}$ cells have differentiated into potent killer cells, but $CD25^{hi}$ cells are more advanced in their effector differentiation.

$CD25^{hi}$ Effector Cells Rapidly Proliferate and Preferentially Generate $KLRG\text{-}1^{hi}$ TE Cells

Differences in effector phenotypic properties of $CD25^{hi}$ and $CD25^{lo}$ $CD8^+$ T cells prompted us to examine whether their differentiation program was different. Because of the well-known effects of IL-2 on cell proliferation and death, we analyzed the extent of cell division and apoptosis induction in $CD25^{hi}$ and $CD25^{lo}$ cells after their purification and adoptive transfer into infection-matched recipients (Figure 4A). This ensured that all environmental cues were maintained similarly to the donor mice, and the donor subsets only differed in their cell intrinsic properties associated with differential CD25 expression.

First, we examined the "take" of both subsets by quantifying the $CD25^{lo}$ and $CD25^{hi}$ donor cells in various lymphoid and nonlymphoid tissues 8 hr after adoptive transfer. Overall, the total number of engrafted donor cells was largely similar for $CD25^{lo}$ and $CD25^{hi}$ subsets at 8 hr after transfer (Figure S3). However, modestly higher numbers of $CD25^{lo}$ cells localized in the lymph nodes, and $CD25^{hi}$ donors exhibited a slight enrichment in peripheral lung and liver tissues.

In order to follow early proliferation of the segregated effector subsets, the sorted donor cells were labeled with CFSE prior to adoptive transfer, and the extent of CFSE dilution was analyzed at days 1.5 and 5 after transfer. Analysis of CFSE dilution at day 1.5 revealed that $CD25^{hi}$ donor cells were dividing more rapidly than the $CD25^{lo}$ cells (Figure 4B). In all tissues examined, $CD25^{hi}$ cells had diluted CFSE more than $CD25^{lo}$ cells and exhibited at least one extra division. This greater proliferation of $CD25^{hi}$ cells correlated with an increased number of $CD25^{hi}$ cells (~5-fold higher) in all tissues examined, compared to $CD25^{lo}$ cells at 1.5 day after transfer (Figure 4B). By day 5 after transfer, both subsets had completely diluted the CFSE, demonstrating that both subsets had divided >10 rounds after transfer (Figure 4C). At this time, the cell number ratios of $CD25^{lo}$ and $CD25^{hi}$ donors were reversed, such that absolute numbers of $CD25^{lo}$ cells were 2- to 5-fold greater than $CD25^{hi}$ cells in all tissues examined (Figure 4C). The decreased numbers of $CD25^{hi}$ donor cells correlated with increased apoptosis of $CD25^{hi}$ cells

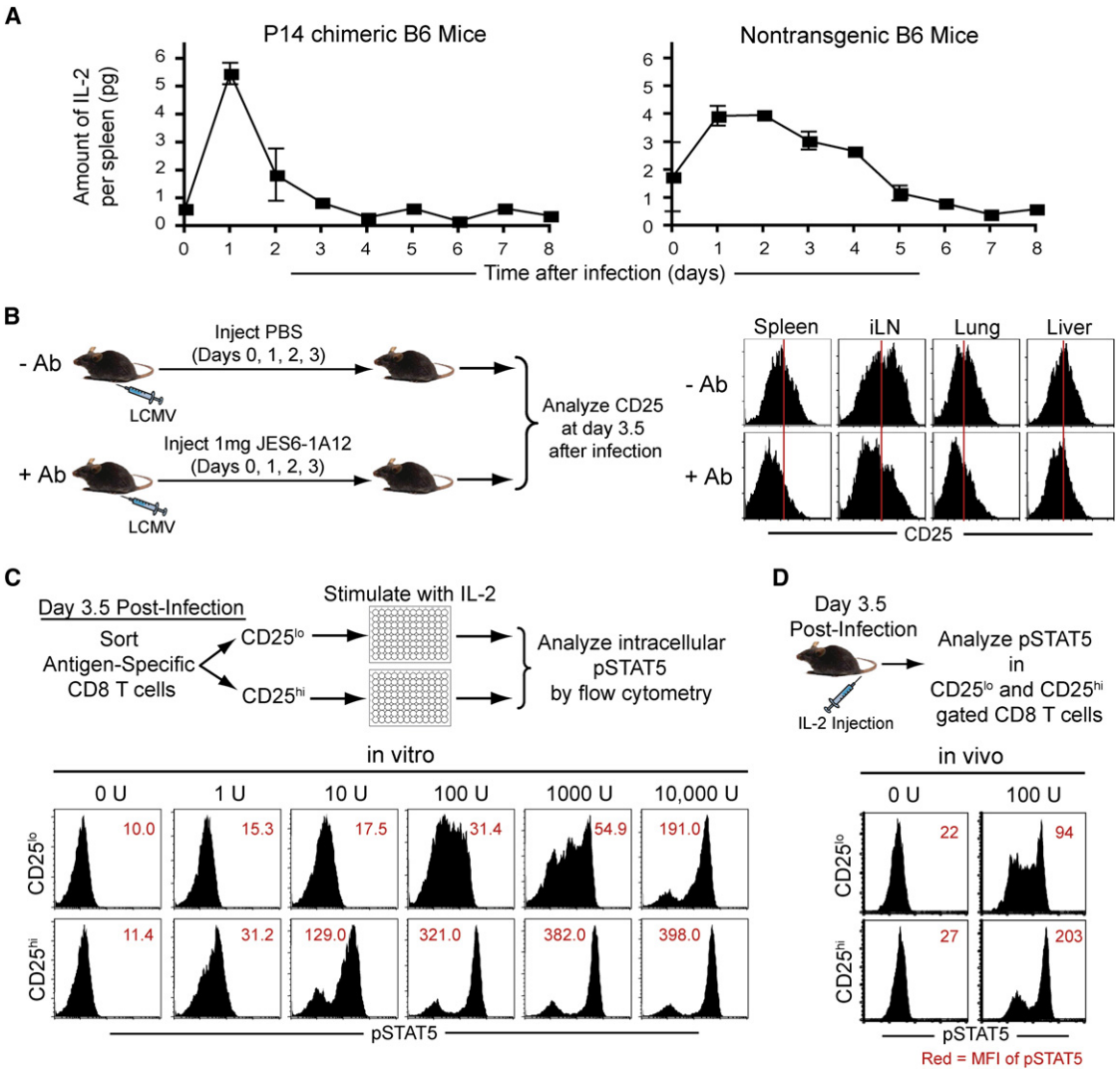

Figure 2. Splenic IL-2 Concentrations and IL-2 Signal Transduction

(A) B6 mice containing 1 × 10^6 P14 cells, or nonchimeric B6 mice, were infected with LCMV and spleens harvested at days 0–8 after infection. Kinetics of IL-2 production in spleen were plotted as amount of IL-2 (pg)/spleen at different days after infection. Symbol indicates mean ± SEM, n = 3. The plot is representative of two independent experiments.

(B) Two groups of 1 × 10^6 P14 chimeric mice were infected with LCMV. One group was treated with 1 mg of blocking IL-2 antibody (JES6-1A12) by intraperitoenal injections at days 0–3. The second control group was injected with PBS. Mice were sacrificed at day 3.5 after infection, and CD25 expression was analyzed on $CD8^+$ $Thy1.1^+$ cells from spleen, inguinal lymph nodes (iLN), lung, and liver. Representative flow cytometry plots from two independent experiments; n = 3 are presented.

(C) $CD8^+$ T cells expressing low or high amounts of CD25 were purified and stimulated in vitro with indicated doses of r-hIL-2 for 15 min. Phosphorylation of STAT5 was assessed by flow cytometry and mean fluorescence intensity (MFI) of pSTAT5 is presented in red.

(D) P14 chimeric mice, containing 1 × 10^6 GP33-specific transgenic cells, were injected with r-hIL-2 after 3.5 days of acute infection. Mice were sacrificed 15 min later, and intracellular p-STAT5 was assessed by flow cytometry. Day 3.5-infected mice that were administered PBS alone were used as a source of unstimulated cells. Histogram plots are representative of two independent experiments; n = 3 for in vitro and in vivo IL-2 stimulation experiments.

compared to $CD25^{lo}$ cells (Figure 4D). Greater frequency of Annexin V^+ $CD25^{hi}$ cells was observed at days 1.5 and 5.0 after transfer (Figure 4D and data not shown). These data demonstrate that $CD25^{hi}$ cells undergo greater extent of proliferation immediately after transfer, but are also more prone to apoptosis.

We next analyzed the expression of granzyme B and KLRG-1 on donor cells after adoptive transfer (Figure 4E). Increased expression of granzyme B and KLRG-1 is associated with effector $CD8^+$ T cells that are more advanced in their differentiation status (Sarkar et al., 2008). We observed increased generation of KLRG-1^{hi} TE cells from $CD25^{hi}$ cells and preferential generation of KLRG-1^{int} MP cells from $CD25^{lo}$ effectors (Figure 4E). $CD25^{hi}$ donor cells expressed higher amounts of granzyme B at the time of sort (Figure 3), and these cells continued to exhibit increased granzyme B expression up to 5 days after adoptive transfer (Figure 4E). This is consistent with previous reports that IL-2 signals regulate the expression of granzyme B (Janas et al., 2005; Liu et al., 1989). Collectively, these data

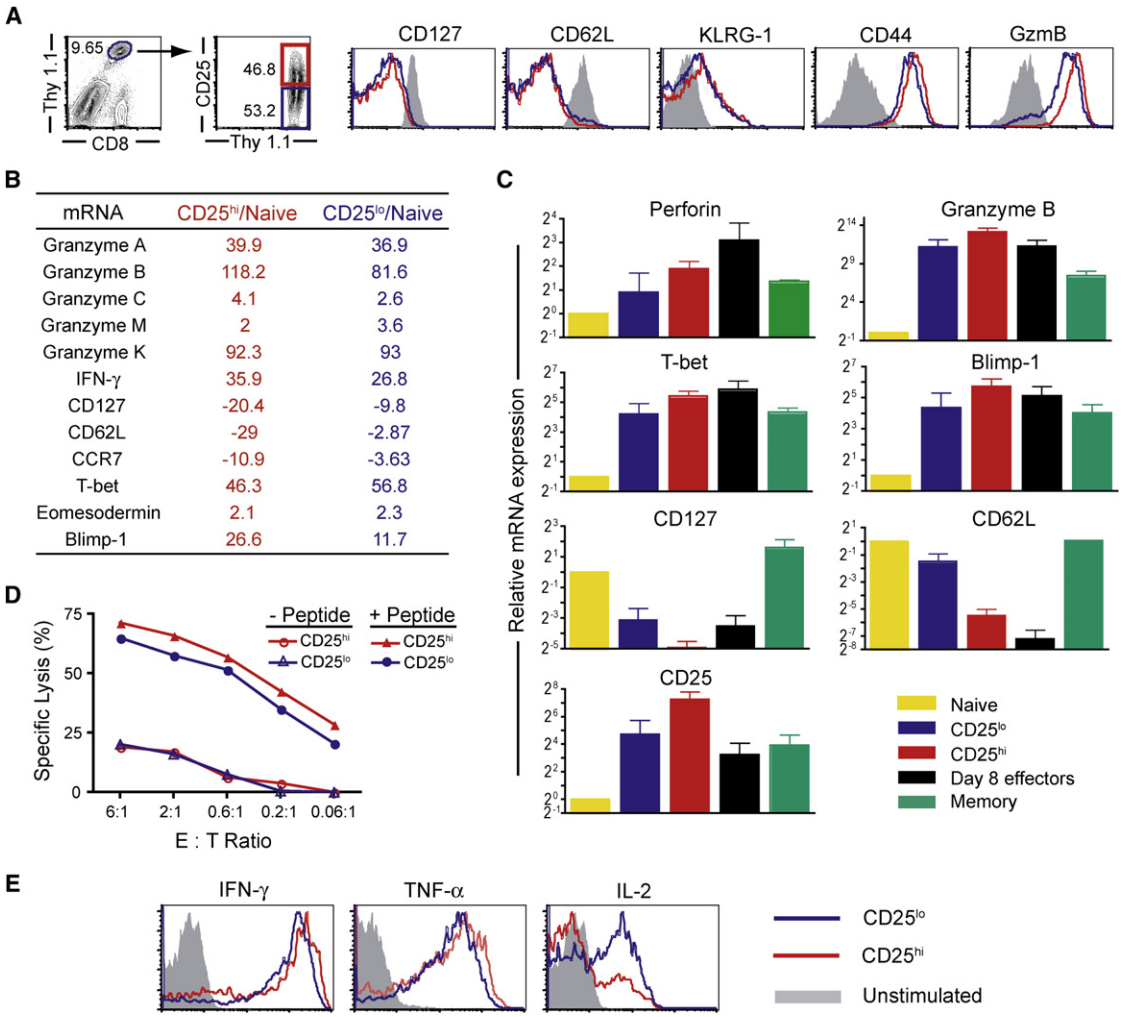

mRNA	CD25hi/Naive	CD25lo/Naive
Granzyme A	39.9	36.9
Granzyme B	118.2	81.6
Granzyme C	4.1	2.6
Granzyme M	2	3.6
Granzyme K	92.3	93
IFN-γ	35.9	26.8
CD127	-20.4	-9.8
CD62L	-29	-2.87
CCR7	-10.9	-3.63
T-bet	46.3	56.8
Eomesodermin	2.1	2.3
Blimp-1	26.6	11.7

Figure 3. Phenotypic and Functional Comparison of CD8+ T Cells Expressing Differential Amounts of IL-2Rα

(A) D^bGP33-specific $CD8^+$ T cells isolated from P14 chimeric mice at day 3.5 postinfection were analyzed for cell surface expression of indicated markers with respect to CD25. $CD8^+$ $Thy1.1^+$ P14 cells were distinguished into $CD25^{hi}$ (red) and $CD25^{lo}$ (blue) cells on the basis of their cell-surface CD25 expression, and expression of indicated surface markers CD127, CD62L, KLRG-1, and CD44 was determined. Direct ex vivo granzyme B expression in $CD8^+$ $Thy1.1^+$ $CD25^{hi}$ and $CD25^{lo}$ $CD8^+$ T cells was assessed by intracellular staining. Gray histograms represent naive controls. Representative data from three independent experiments are presented.

(B and C) $CD25^{hi}$ and $CD25^{lo}$ $CD8^+$ T cells were purified from day 3.5 LCMV-infected splenocytes and mRNA isolated, and expression of transcripts for the indicated molecules analyzed. Data are presented as fold increase or decrease (depicted by negative numbers) over naive and are representative of three to four independent replicates. Data in (B) are from affymetrix gene chip analyses, and in (C) are from RT-PCR analyses with specific primers to detect indicated mRNAs. Data are presented as fold over naive with naive mRNA levels normalized to 1.

(D) Cytotoxicity mediated by purified $CD25^{hi}$ and $CD25^{lo}$ cells was analyzed by standard 5 hr Cr^{51} release assay with GP33-coated target cells. Target cells that were not coated with peptide (– Peptide) were used as negative controls.

(E) Splenocytes were isolated from P14 chimeric mice at day 3.5 after LCMV infection. $CD8^+$ T cells expressing high and low CD25 were purified and stimulated in vitro with GP33 peptide for 5 hr in the presence of brefeldin A. IFN-γ, TNF-α, and IL-2 production was assessed thereafter by intracellular cytokine staining. Unstimulated cultures were used as negative controls (gray histograms). Data presented are representative of three different experiments with two to three mice per group.

demonstrate that $CD25^{hi}$ cells undergo rapid proliferation compared to $CD25^{lo}$ cells, exhibit increased apoptosis, and predominantly differentiate into KLRG-1^{hi} TE cells. Thus, early heterogeneity in CD25 expression marks a differential developmental program in $CD8^+$ T cells, such that cells that maintain prolonged CD25 expression and thereby receive comparatively more IL-2 signals are more likely to differentiate into TE cells.

$CD25^{lo}$ Cells Preferentially Upregulate L-Selectin and Differentiate into Long-Lived Functional Memory Cells

To determine the eventual memory potential of $CD25^{hi}$ and $CD25^{lo}$ effector subsets, and to evaluate the quality of memory cells arising from both effector subsets, we purified $CD25^{hi}$ and $CD25^{lo}$ effector cells by flow cytometry at day 3.5 after infection, transferred them in equal numbers to congenic hosts, and

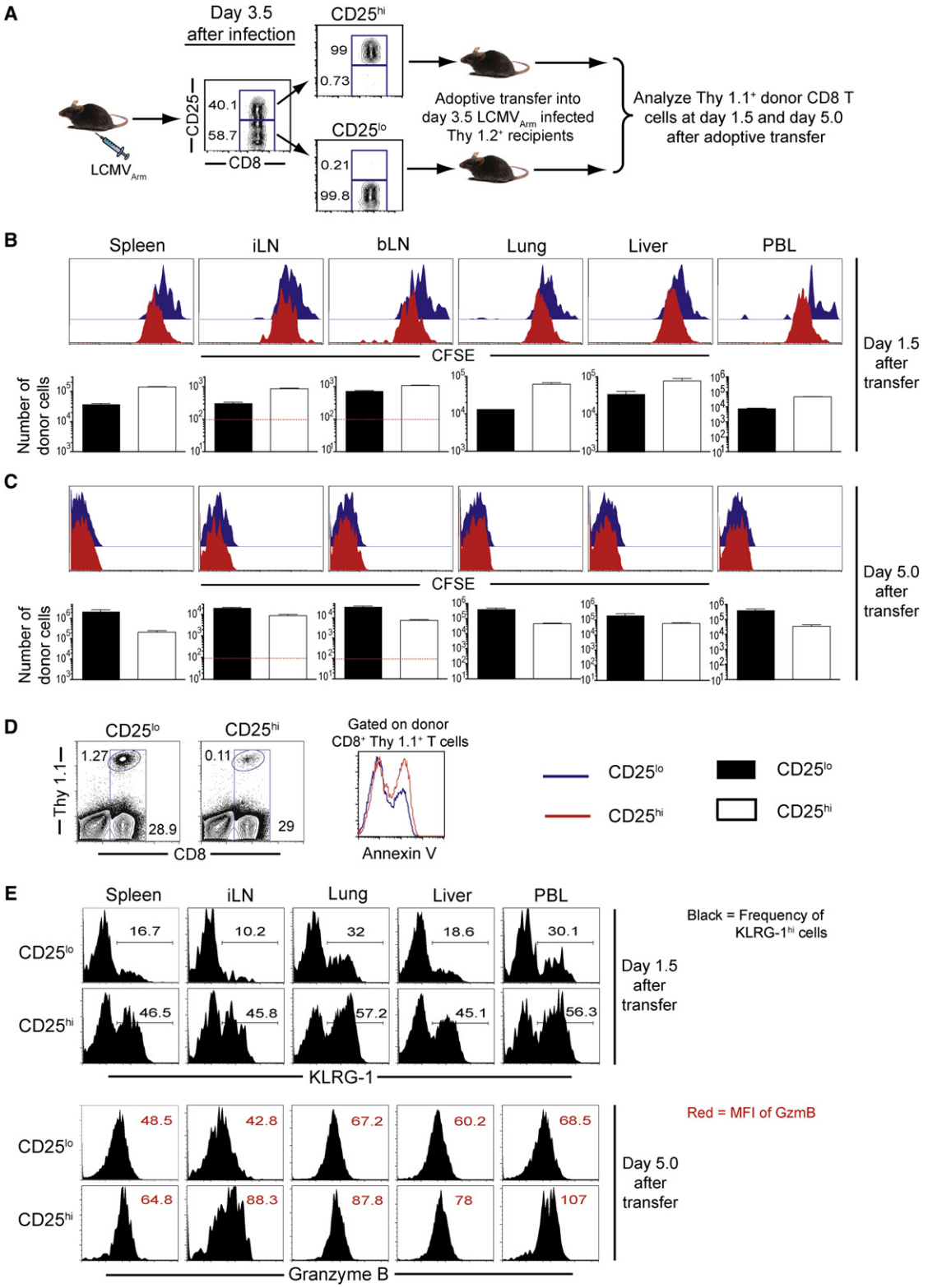

Figure 4. Proliferation, Survival, and Differentiation of CD25^{hi} and CD25^{lo} CD8^{+} T Cells

(A–C) As shown in (A), CD25^{hi} and CD25^{lo} cells were purified by flow cytometry at day 3.5 after infection and labeled with CFSE, and equal numbers were adoptively transferred into infection-matched recipients. Donor cells were tracked in Thy1.2^{+} recipient mice with the congenic marker Thy1.1. Absolute numbers of donor cells were determined in spleen, inguinal lymph nodes (iLN), brachial lymph nodes (bLN), lung, liver, and peripheral blood lymphocytes (PBL) at ~1.5 days

followed acquisition of key memory properties such as long-term maintenance of donor cells, upregulation of lymph node-homing marker CD62L, IL-2 production, and recall proliferation potential.

The kinetics of donor cell expansion, contraction, and maintenance were determined by assessment of $CD8^+$ $Thy1.1^+$ donor cells longitudinally (Figure 5A) in blood and in various tissues at day 180 after transfer (Figure 5B). After adoptive transfer, both $CD25^{hi}$ and $CD25^{lo}$ subsets underwent substantial expansion. However, consistent with data in Figure 4B, $CD25^{hi}$ cells apparently exhibited enhanced expansion during first 2 days after transfer. With respect to memory outcome, as predicted by preferential generation of KLRG-1^{int} MP cells from $CD25^{lo}$ cells, the $CD25^{lo}$ donors persisted at ~5-fold higher numbers than $CD25^{hi}$ donors in blood after contraction (Figure 5A). Similarly, $CD25^{lo}$ donor cells gave rise to ~5-fold higher absolute numbers of long-lived memory cells in all lymphoid and nonlymphoid tissues tested (Figure 5B and Figure S4A).

L-selectin is classically employed as a key memory marker that distinguishes long-lived memory cells capable of preferential migration to lymph nodes. We found that $CD25^{lo}$ donor cells not only exhibited preferential survival into memory phases but were also capable of upregulating CD127 and L-selectin, phenotypic markers associated with long-lived memory cells, more efficiently than $CD25^{hi}$ donor cells after antigen clearance (Figure 5C and Figure S4B). Although the majority of $CD25^{lo}$ donor cells had upregulated CD62L expression by day 120 after transfer, the few $CD25^{hi}$ donor cells that survived into memory phases exhibited a compromised ability to upregulate CD62L and CD127. Consistent with higher CD62L expression, memory cells arising from $CD25^{lo}$ donor cells also exhibited increased localization in lymph nodes compared to $CD25^{hi}$ donor cells (Figure S4C).

In addition to more efficient acquisition of classic memory phenotype by $CD25^{lo}$ donor cells, these cells also exhibited various functional attributes of optimal memory cells. Although both donor subtypes produced similar amounts of IFN-γ and TNF-α, memory cells arising from $CD25^{lo}$ donors were capable of superior IL-2 production, compared to memory cells from $CD25^{hi}$ donors (Figure 5D).

Robust recall proliferation upon secondary challenge is a hallmark property of memory cells. To examine recall responses, we isolated memory cells arising from $CD25^{lo}$ and $CD25^{hi}$ donors, adoptively transferred equal numbers into naive mice, and challenged these mice with recombinant vaccinia virus expressing the GP33 epitope of LCMV. Expansion of $CD8^+$ $Thy1.1^+$ donor cells was assessed by quantification of the absolute number of donor cells in spleen of challenged mice at 5.5 days after infection. In this test of memory cell functionality, we observed that memory cells arising from $CD25^{lo}$ donors expanded to a greater extent (~5-fold greater increase) and were able to mount a more robust recall proliferation compared to $CD25^{hi}$ donor cells (Figure 5E). These data clearly demonstrate that early during priming, the heterogeneity in CD25 expression distinguishes diverse memory fates, such that long-lived functional memory cells preferentially arise from effector $CD8^+$ T cells that downregulate CD25 expression earlier.

$CD25^{hi}$ Lineage Maintains Qualitative Imprinting Even When $CD8^+$ T Cell Stimulation Is Curtailed

In the above experiments, we followed the fate of $CD25^{hi}$ and $CD25^{lo}$ cells in infection-matched recipients as it normally occurs during an infection. Next, we sought to analyze the memory outcome of $CD25^{hi}$ and $CD25^{lo}$ cells in an environment where there was minimal IL-2. Thus, we performed a similar sort and adoptive transfer experiment as described above with the difference that LCMV immune mice were used as recipients of $CD25^{hi}$ and $CD25^{lo}$ effector cells. LCMV immune recipients (mice that had cleared the infection several months earlier) provided an in vivo environment with minimal IL-2 and TCR signals compared to infection-matched recipients used in the previous experiments. Moreover, as opposed to naive recipients, memory mice also provided the unique advantage of rapidly controlling any virus that may be transferred such that both IL-2 and TCR signals (and other infection-induced signals) would be blunted upon transfer. This allowed us to examine whether the fate of $CD25^{hi}$ and $CD25^{lo}$ cells was already programmed at the time of sort or whether it was continuously modulated toward later stages of infection.

A longitudinal analysis of $CD25^{hi}$ and $CD25^{lo}$ donor cells in the blood of LCMV immune recipients was performed. Subsequently, absolute donor cell numbers in different tissues were also assessed at memory time point. After adoptive transfer, as expected, both $CD25^{hi}$ and $CD25^{lo}$ donor cells continued to expand as they were already cycling (Figure 6A). However, in the absence of further TCR and IL-2 signals, the numbers of $CD25^{hi}$ and $CD25^{lo}$ donor cells did not continue to increase until day 5 after transfer, as was the case with infection-matched recipients. Contraction ensued day 1 after transfer, and after contraction $CD25^{hi}$ cells persisted at ~5-fold higher numbers than $CD25^{lo}$ cells in the blood. Similarly, $CD25^{hi}$ donor cells were present at 5- to 10-fold higher numbers than $CD25^{lo}$ cells in all tissues analyzed (spleen, inguinal and brachial lymph nodes, lung, and liver) (Figures 6B and 6C). The higher numbers of $CD25^{hi}$ donor cells at memory correlated with higher numbers at day 1 after adoptive transfer. This is consistent with data in Figure 4 in which $CD25^{hi}$ cells were found to undergo rapid proliferation compared to $CD25^{lo}$ cells. In the absence of continued IL-2 signals, this rapid proliferation of $CD25^{hi}$ donor cells is presumably not accompanied by enhanced apoptosis that was observed in infection-matched recipients, thereby accounting

(B), and 5 days (C) after transfer for assessment of $CD8^+$ T cell expansion. At these time points, extent of proliferation of $CD25^{hi}$ (red) and $CD25^{lo}$ (blue) donor cells was also assessed by determining their CFSE dilution profile in indicated tissues.

(D) Apoptosis of donor subsets was evaluated in day 5 splenocytes by measuring the percentage of Annexin V^+ cells. Representative raw data depicting the percentage of $CD8^+$ $Thy1.1^+$ donor cells are also presented.

(E) Expression of KLRG-1 and granzyme B on $CD25^{hi}$ and $CD25^{lo}$ donor cells were assessed in indicated tissues at day 1.5 and 5.0 after adoptive transfer into infection-matched recipients, respectively. Representative histogram plots for KLRG-1 and granzyme B expression are presented. Data are representative of two independent experiments with two to three replicates. Numbers within the histogram plots indicate the percentage of KLRG-1^+ cells and the MFI of granzyme B expression.

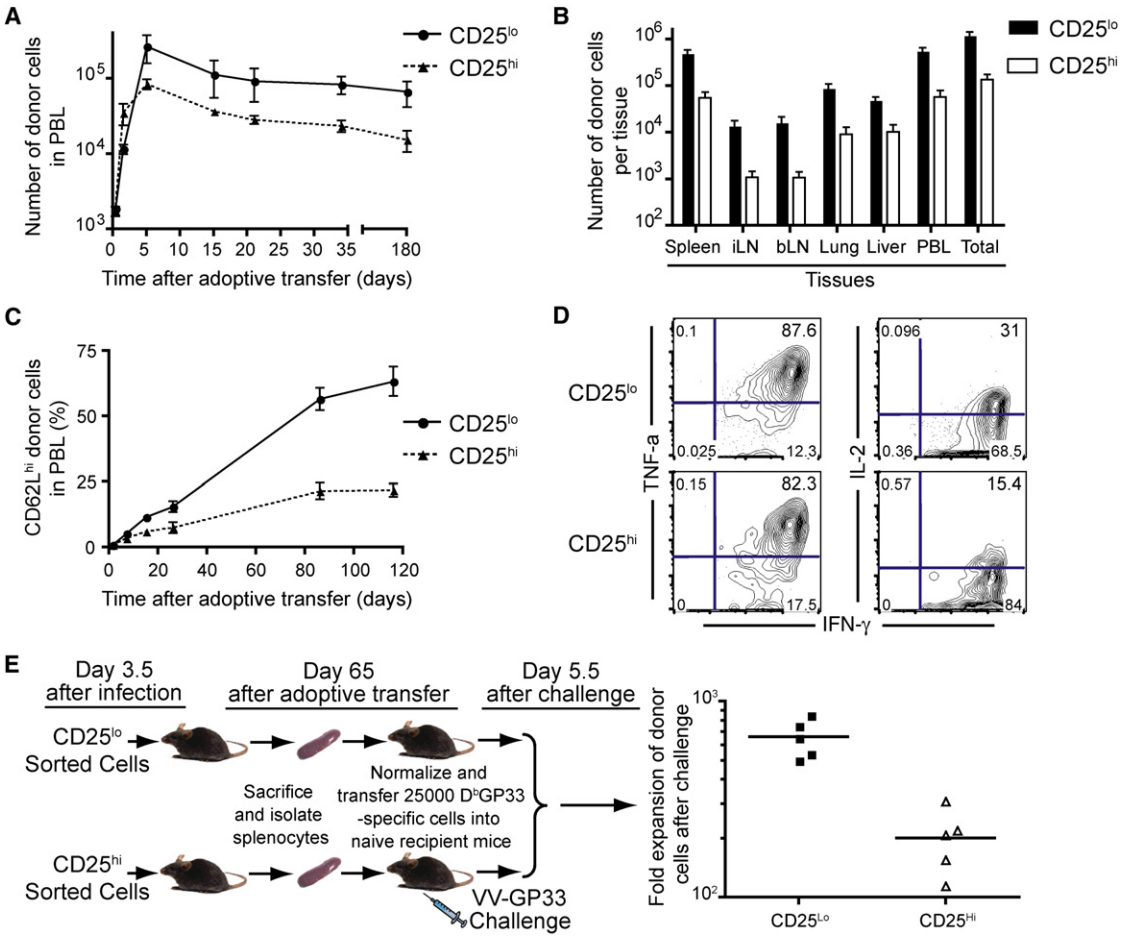

Figure 5. Memory Differentiation of Effector CD8+ T Cells Expressing Differential Levels of CD25 during Priming

$CD25^{hi}$ and $CD25^{lo}$ cells were purified by flow cytometry, and equal numbers were adoptively transferred into infection-matched recipients, as in Figure 4. Donor cells were tracked in recipient mice with the congenic marker Thy1.1.

(A) Kinetics of donor cell proliferation and contraction in blood were determined by assessment of the number of $CD8^+$ Thy1.1 cells per 10×10^6 PBL at various time points after transfer. Line graph summarizes mean number of donor cells ± SEM from five independent experiments with one to three mice per group.

(B) Absolute numbers of donor cells were enumerated in the indicated lymphoid and nonlymphoid tissues at 180 days after transfer. Summary graphs of mean donor cell numbers ± SEM are plotted for five to eight recipient mice. Donor cells in PBL are plotted per 10×10^6 cells.

(C) $CD8^+$ $Thy1.1^+$ donor cells were analyzed for the expression of lymphoid homing marker CD62L in blood. Average values of percentage $CD62L^+$ $CD25^{lo}$ and $CD25^{hi}$ donor cells are presented at different days after sort and transfer. Error bars represent ± SEM.

(D) Splenocytes from $CD25^{hi}$ and $CD25^{lo}$ recipient mice were isolated at day 65 after transfer and stimulated in vitro with GP33 peptide for 5 hr, after which IFN-γ, TNF-α, and IL-2 production by $CD8^+$ $Thy1.1^+$ donor cells was assessed by intracellular cytokine staining. Numbers in each quadrant indicate frequencies that are of $CD8^+$ $Thy1.1^+$ donor cells within the quadrant and that are based on IFN-γ, TNF-α, or IL-2 stainings.

(E) Memory cells generated from day 3.5 $CD25^{hi}$ and $CD25^{lo}$ purified effector cells were isolated from spleen 65 days after transfer and column purified, and equal numbers of $CD8^+$ $Thy1.1^+$ donors were adoptively transferred into naive mice. Extent of proliferation after secondary challenge with recombinant vaccinia virus expressing GP33 was assessed by enumeration of $CD8^+$ $Thy1.1^+$ donor cells in spleen. Data are presented as fold increase of donor cells with respect to input cells. Each symbol represents an independent mouse and each bar represents average fold expansion for the group.

for their greater accumulation. However, the phenotype of memory cells arising from $CD25^{hi}$ donor cells was similar in both infection-matched and LCMV immune recipients. Thus, $CD25^{hi}$ donor cells exhibited lower expression of CD127 and CD62L and higher expression o KLRG-1 (Figure 6D). Functionally, memory cells arising from $CD25^{hi}$ donor cells produced less IL-2 compared to $CD25^{lo}$ donors when transferred into LCMV immune mice or infection-matched recipients (Figure 6E).

Collectively, these studies demonstrate that the heterogeneity in CD25 expression marks a differential memory program in effector cells, such that $CD25^{lo}$ effectors differentiate into long-lived functional memory cells that upregulate CD62L, produce IL-2, and mount a robust recall response. In contrast, effector cells that maintain CD25 expression for longer periods are driven toward terminal differentiation and give rise to memory cells with suboptimal functional properties.

Prolonged IL-2 Signals Contribute to Terminal-Effector Differentiation

To directly test the hypothesis that prolonged IL-2 signals drive terminal-effector differentiation, we exogenously administered high doses of IL-2 (30,000 U/mouse/day) during the expansion

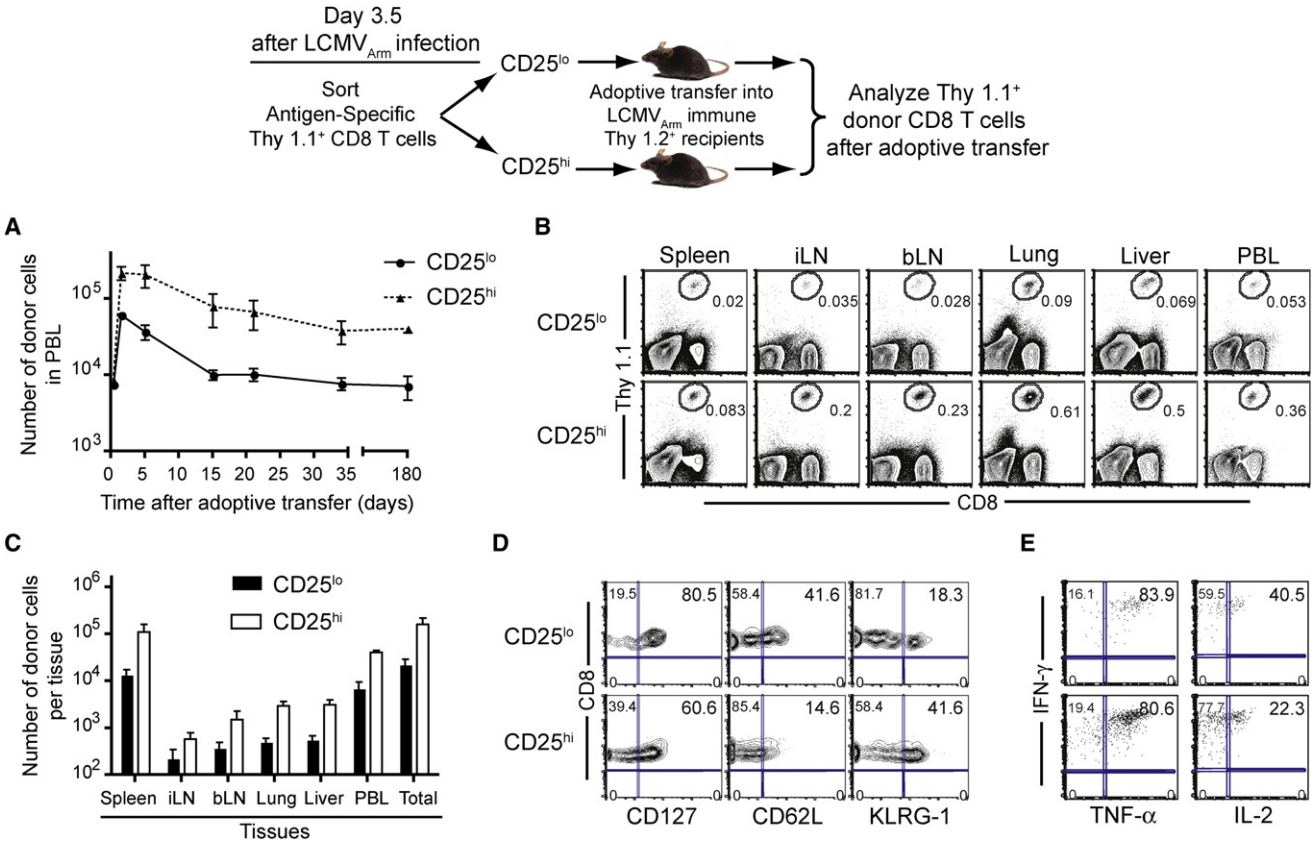

Figure 6. Memory Outcome of Effector CD8+ T Cells Expressing Differential Amounts of CD25 upon Curtailment of IL-2 Signals

(A) CD25hi and CD25lo cells were purified at day 3.5 after infection, and equal numbers were adoptively transferred into LCMV immune recipients. Donor cells were tracked in recipient mice with the congenic marker Thy1.1. Kinetics of donor cell expansion and contraction in blood were determined by assessment of the number of CD8+ Thy1.1+ donor cells per 10 × 10^6 peripheral blood lymphocytes at various time points after transfer. Mean ± SEM donor cell numbers per 10 × 10^6 PBL are shown at indicated time points after adoptive transfer.

(B and C) Absolute numbers of donor cells were enumerated in the indicated lymphoid and nonlymphoid tissues at 180 days after transfer. Representative raw data (B) and summary graphs (C) are presented for three recipient mice. Bar graphs represent mean ± SEM of donor cell numbers in indicated tissues.

(D) CD8+ Thy1.1+ donor cells were analyzed for the expression of the indicated phenotypic markers in blood at day 30 after transfer. Flow cytometry raw data representative of three mice are presented.

(E) Splenocytes from CD25hi and CD25lo recipient mice were isolated at day 180 after transfer and IFN-γ, TNF-α, and IL-2 production by CD8+ Thy1.1+ donor cells was assessed by intracellular cytokine staining after in vitro GP33 peptide stimulation. Numbers indicate percentage of donor cells in each quadrant.

phase of CD8+ T cell response (days 0–8 after infection). At this dose of IL-2, both CD25lo and CD25hi effector cells transduced high amounts of intracellular IL-2 signals as determined by STAT5 phosphorylation (data not shown). CD8+ T cell expansion, contraction and extent of effector differentiation were analyzed thereafter by quantification of the absolute numbers of antigen-specific cells and by assessment of granzyme B expression, respectively. The prediction was that under conditions in which all antigen-specific cells receive prolonged IL-2 signals, CD8+ T cell differentiation will be skewed toward terminal-effector cell fate. Both GP33- and NP396-specific CD8+ T cells from IL-2-treated mice expressed higher amounts of granzyme B in all tissues examined, compared to untreated control mice (Figures 7A and 7B). These data are consistent with increased granzyme B expression by CD25hi cells and demonstrate increased effector differentiation in presence of enhanced IL-2 signals. Moreover, consistent with previous reports (Blattman et al., 2003), IL-2 treatment during the expansion phase resulted in increased CD8+ T cell expansion and contraction as depicted by antigen-specific CD8+ T cell numbers at peak of expansion (day 8) and after contraction (day 15) (Figure S5). These observations are similar to data in Figure 5, in which CD25hi cells capable of receiving enhanced IL-2 signals tend to expand and contract more than their CD25lo counterparts.

Genome-wide Microarray Analysis of Effector Cells Programmed toward Memory versus Terminal-Effector Fates

The evident differences in functional properties and memory fates of CD25lo and CD25hi CD8+ T cells prompted us to perform a genome-wide microarray analysis of both subsets to delineate in detail the genes that are differentially expressed. This knowledge may be useful in understanding the early signals that are important in driving TE versus MP lineage choices. Thus, we purified CD25lo MP and CD25hi TE CD8+ T cells from day 3.5 and performed gene chip analyses of both subsets, relative to naive cells.

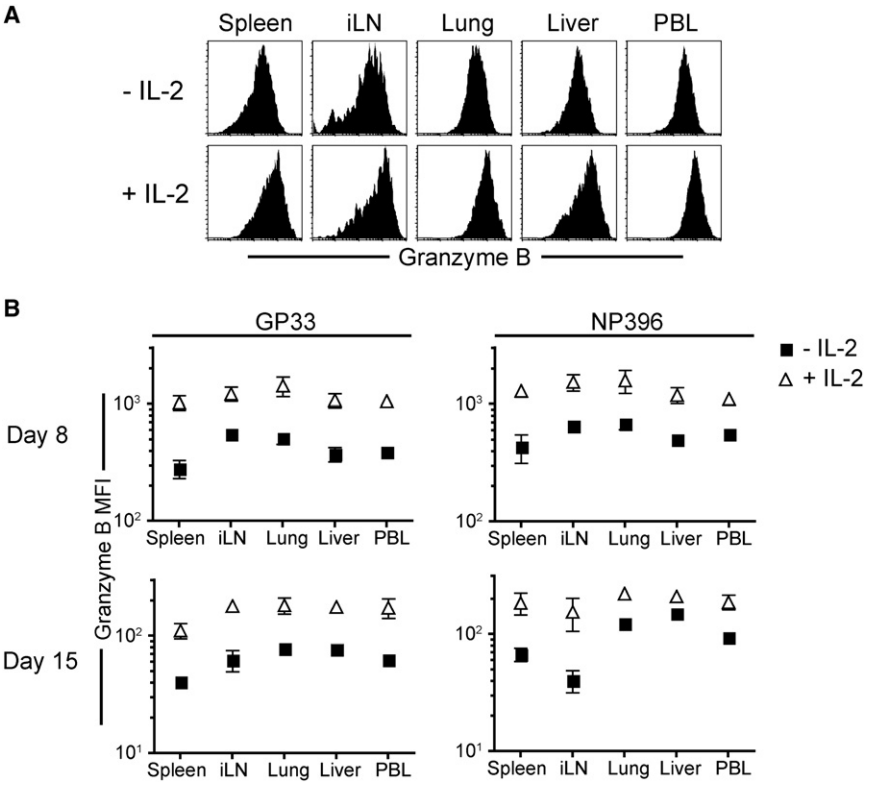

Figure 7. CD8+ T Cell Responses after In Vivo IL-2 Administration

(A) Naive C57Bl/6 mice were infected with LCMV. One set of mice was injected with high dose of IL-2 (15,000 U/mouse) intraperitoneally twice a day from days 0–8 after infection. Control mice received PBS injections. The extent of effector differentiation was evaluated by measurement of granzyme B expression in D^bGP33- and D^bNP396-specific cells isolated from indicated tissues at days 8 and 15 after infection with anti-CD8α, anti-granzyme B and respective MHC-I tetramers. Representative raw data for granzyme B expression by D^bGP33-specific $CD8^+$ T cells at day 8 after infection are presented in (A). Average MFI of granzyme B expression by D^bGP33- and D^bNP396-specific $CD8^+$ T cells at days 8 and 15 postinfection are plotted in (B). Plots summarize two independent experiments with three replicates each, and error bars represent SEM.

Compared to naive cells, both $CD25^{hi}$ and $CD25^{lo}$ subsets exhibited differential expression (upregulation or downregulation) of ~4000 genes—$CD25^{hi}$ cells differentially expressed ~4099 genes relative to naive cells, and $CD25^{lo}$ $CD8^+$ T cells had upregulated or downregulated the expression of ~3786 genes compared to naive cells. Between both subsets, ~720 genes were differentially expressed. Out of these 720 differentially regulated genes, 530 genes were expressed at relatively higher levels in $CD25^{lo}$ cells compared to $CD25^{hi}$ cells.

Compared to naive cells, both $CD25^{lo}$ and $CD25^{hi}$ $CD8^+$ T cells upregulated the expression of several effector genes including granzymes A, B, C, M, and K, IFN-γ, T-bet, eomesodermin, and Blimp-1. However, it is noteworthy that $CD25^{hi}$ cells expressed modestly higher amounts of most of these effector genes (Figure 3 and Table S1). Stress proteins (heat-shock proteins, growth arrest 5) were also expressed at higher amounts in $CD25^{hi}$ cells. Consistent with the observation that $CD25^{hi}$ cells divide more, $CD25^{hi}$ cells expressed cell cycle genes to a higher extent compared to $CD25^{lo}$ cells (proliferation-associated 2G4, S-phase kinase-associated protein 2) (Figure S6A and Table S1). Although effector genes were expressed at higher amounts in $CD25^{hi}$ cells, genes that are known to repress terminal differentiation (*Bcl6*) were expressed at higher amounts in $CD25^{lo}$ cells (Table S1). As expected for effector cells, both subsets had also downregulated lymph node-homing molecules CD62L and CCR7, as well as IL-7Rα, albeit to different levels—$CD25^{hi}$ cells exhibited increased downregulation of *Cd62l*, *Ccr7*, and *Cd127* compared to $CD25^{lo}$ cells. Combined with the observations of similar CTL potential of $CD25^{lo}$ and $CD25^{hi}$ cells, these analyses demonstrate that similar to TE cells, memory-fated $CD8^+$ T cells also pass through an effector phase.

MP cells exhibited increased expression of several cell survival genes, including *Bcl-2*, *Parp-3*, and *Spi-2a*, as well as key players of signaling networks involved in promoting cell survival (*Jak1*, which acts upstream of AKT, and *Cd40* and *Relb*, participating in alternative NF-κB pathway induction) (Table S1). These observations are consistent with increased survival of $CD25^{lo}$ memory precursors following adoptive transfer.

Several pathways of innate signaling were found to be higher in MP cells than TE cells (Figure S6B and Table S1). The innate genes and pathways that were selectively overexpressed in MP cells compared to TE cells included (1) type I interferon pathway, such as *Ifn-r1*, *Ifn-r2*, *Jak1*, *Stat1*, *Ifit1*, and *Ifit3* (interferon induced protein with tetratricopeptide repeats); (2) IL-6 signaling pathway including *Il-6r* and IL-6 signal transducer; (3) direct expression of Toll-like receptors *Tlr-1* and *Tlr-3*, which are typically expressed on cells of the innate immune system; (4) TNF signaling pathway genes including *Traf1* (TNF-receptor associated factor 1), *Tnfaip8l2*, and *Traf3ip3*; and (5) NF-κB signaling (*Pkr*, *Pkc*, *Malt1*, and *Relb*). Such a concerted overexpression of genes involved in innate signaling in MP relative to TE cells is consistent with the known function of innate signals in promoting effector differentiation.

DISCUSSION

Previous reports have demonstrated the significance of IL-2 signals in modulating $CD8^+$ T cell responses. However, evidence exists in favor of both positive and negative impact of IL-2 on $CD8^+$ T cell memory development (Blattman et al., 2003; Cheng and Greenberg, 2002; Cheng et al., 2002; Williams et al., 2006). By following the kinetics of CD25 expression in vivo after LCMV infection, and by determining the fate of $CD8^+$ T cells expressing differential levels of CD25, our studies reconcile both reports. Consistent with the proposal of Williams et al. (2006) that IL-2 signals are important for the generation of functional memory

cells, we find that early after infection, all CD8+ T cells upregulate the expression of high-affinity IL-2Rα similarly. These cells are thus capable of perceiving IL-2 signals in vivo, which may be crucial for antigen-independent expansion (Kaech and Ahmed, 2001), effector cell differentiation, and possibly programming of memory potential. Thereafter, a transient heterogeneity in CD25 expression appears, which correlates with differential memory outcomes—cells that are capable of perceiving prolonged IL-2 signals are represented less in the long-lived memory pool, whereas cells that downregulate CD25 earlier preferentially contribute to the long-lived functional lymphoid memory pool. Consistent with previous reports (Blattman et al., 2003), $CD25^{hi}$ cells that retain elevated expression of CD25 longer tend to undergo enhanced expansion that is coupled with greater cell death. This is largely governed by the duration of IL-2 and other infection-related stimuli (antigen and inflammation, for example), such that prolonged stimulation drives $CD25^{hi}$ cells toward terminal-effector differentiation. These data are supportive of a linear continuum of effectors that differentiate into lymphoid memory cells, nonlymphoid memory cells, or terminal effectors on the basis of the degree of stimulation perceived.

How is CD25 expression regulated? The expression kinetics of CD25 follows viral replication. At days 1–2 after infection, when virus is replicating exponentially, all virus-specific cells are likely to encounter antigen. This prediction is consistent with uniform upregulation of CD25 expression by antigen-specific CD8+ T cells. Thereafter, at around day 3.5–4 after infection, when antigen-specific CD8+ T cells have greatly expanded and antigen is decreasing, stochastic encounter of a subset of T cells with limiting antigen may be responsible for heterogeneous expression of CD25. Finally, around day 6 after infection, when antigen is largely cleared from the system, CD25 expression is uniformly downregulated on antigen-specific CD8+ T cells. $CD25^{hi}$ cells may also selectively localize to antigen-rich niches, thus maintaining higher CD25 expression. IL-2 signals can also directly upregulate CD25 expression. Whereas CD25 expression is regulated by the TCR via an NF-kB site just near the start site, after IL-2 is produced CD25 expression is augmented ~10- to 20-fold via tandem STAT5 sites that are ~9000 bp upstream (Malek, 2008; Smith and Cantrell, 1985). Therefore, the level of CD25 expression is markedly dependent upon the availability and concentration of IL-2. This is supported by our kinetics of splenic IL-2 expression. Additionally, in vivo administration of IL-2 leads to increased CD25 expression on CD8+ T cells (V.K., S.S., and R.A., data not shown, and Blattman et al., 2003). Thus, the observed in vivo heterogeneity in CD25 expression probably results from a combination of differential TCR and IL-2 signals, both an integral part of an acute infection.

The distinct memory outcomes associated with $CD25^{hi}$ and $CD25^{lo}$ effectors clearly correlates with differential IL-2 signaling. This is demonstrated by enhanced phosphorylation of STAT5 in $CD25^{hi}$ cells both in vitro and in vivo. Moreover, consistent with previous reports that Blimp-1 expression is upregulated by increased IL-2 signals (Calame, 2008; Gong and Malek, 2007; Malek, 2008), and that Blimp-1 drives terminal-effector differentiation (Rutishauser et al., 2009), $CD25^{hi}$ cells that are capable of perceiving prolonged IL-2 signals express relatively more Blimp-1 than $CD25^{lo}$ cells. Recent studies (Martins and Calame, 2008; Martins et al., 2008) demonstrate that Blimp-1 directly represses IL-2 and the IL-2 activator Fos. Consistent with this, $CD25^{hi}$ cells that express higher levels of Blimp-1 are significantly impaired in their ability to produce IL-2. Greater granzyme B expression by $CD25^{hi}$ cells is also consistent with increased IL-2 signaling (Janas et al., 2005). In contrast, correlating with their enhanced ability to produce IL-2, $CD25^{lo}$ cells express higher levels of Bcl-6, a key negative regulator of Blimp-1. It is likely that enhanced Bcl-6 expression by MP cells compared to TE cells may exert a role in preventing terminal differentiation in memory fated cells (Manders et al., 2005). How IL-2 signals drive terminal differentiation is intriguing. An accompanying article by Pipkin et al. (2010) in this issue of *Immunity* demonstrates that enhanced expression of perforin by high-dose IL-2 is associated with Stat5 and Eomesodermin recruitment to the *Prf1* locus. It is interesting to speculate whether enhanced IL-2 signals may directly impact CD127 and CD62L reacquisition via epigenetic silencing of the loci or regulation of transcription factors, in addition to promoting the expression of effector genes.

Delineation of MP and TE cells early during an immune response provides us with a tool to further understand the signals that program memory fates. Consistent with previous observations in the field, this early analysis of MP and TE subsets confirms that superior IL-2 production is a unique property of MP cells at different times of differentiation (Joshi et al., 2007; Kaech et al., 2003; Marzo et al., 2005; Sarkar et al., 2008; Wherry et al., 2003). CD8+ T cells have been shown to undergo asymmetric cell division such that unequal apportioning of proteins occurs during the first cell division after priming (Chang et al., 2007), which correlates with differential cell fates. Interestingly, the differences in expression of granzyme B and CD62L between $CD25^{hi}$ and $CD25^{lo}$ effectors shows a similar trend as the proximal and distal daughter cells that arise after the first round of cell division. Additionally, our gene chip analyses reveal a coordinately enhanced expression of innate pathways in MP cells compared to TE cells. This suggests that memory cells differentiate from effector cells and is consistent with the proposal that (Kolumam et al., 2005; Pulendran and Ahmed, 2006) direct action of type I interferons on CD8+ T cells promotes CD8+ T cell expansion and survival, thus resulting in the generation of a stable pool of memory T cells. Collectively, our studies provide insights into the timing and mechanism of action of IL-2 signals in regulating T cell effector and memory differentiation. This information may be useful in rational vaccine design and development of immunotherapeutic strategies.

EXPERIMENTAL PROCEDURES

Mice, Virus, and Infections

C57BL/6 mice (Thy1.2+ or Thy1.1+) were purchased from the Jackson Laboratory (Bar Harbor, ME, USA). Thy1.1+ P14 mice bearing the Db-gp33-specific TCR were fully backcrossed to C57BL/6 and maintained in our animal colony. LCMV Armstrong ($LCMV_{Arm}$), and recombinant vaccinia virus that expresses the GP33 epitope of LCMV (VV-GP33) were propagated, titered and used as described (Kaech et al., 2002; Sarkar et al., 2008). All mice were used in accordance with NIH and the Emory University Institutional Animal Care and Use Committee guidelines.

IL-2, Antibodies, Flow Cytometry, and Intracellular Cytokine Staining

Recombinant human IL-2 used for CD8+ T cell stimulation was kindly provided by K.A. Smith (Cornell University, New York). IL-2 estimation in spleen was performed by Assaygate (Ijamsville, MD, USA). MHC class I peptide tetramers were made and used as described previously (Murali-Krishna et al., 1998). Antibodies and procedures for flow cytometric analysis of surface or intracellular proteins and cytokines have been described previously (Kaech et al., 2002; Sarkar et al., 2008). Intracellular phospho-STAT5 analysis was performed as described previously (Kersh et al., 2003; Krutzik et al., 2005a; Krutzik et al., 2005b).

Isolation of T Cells, Adoptive Transfers, CTL Assays, and CFSE Labeling

Effector Thy1.1+ P14 CD8+ T cells were isolated from spleens of mice infected with anti-CD8+ magnetic beads (Miltenyi Biotec, Auburn, CA, USA) in accordance with the manufacturer's instructions. For additional purification of $CD25^{lo}$ and $CD25^{hi}$ cells, purified CD8+ T cells were stained with anti-CD8α, anti-Thy1.2, and anti-CD25 on ice in PBS containing 1% FCS and were FACS sorted with BD FACS Aria (Becton Dickinson, San Jose, CA, USA). Equal numbers of sorted Thy1.1+ P14 cells (~0.5 to 2.0 × 10^6) were transferred intravenously into infection-matched or LCMV-immune C57BL/6 mice. Donor cells were distinguished with Thy1.1 mAb and isolated from spleen, lymph node, liver, lung, and blood as described (Sarkar et al., 2008). Cells were labeled with CFSE for analyzing cell proliferation after adoptive transfer (Molecular Probes) as described previously (Kaech et al., 2002; Sarkar et al., 2008). GP33-41-specific CTL activity was determined by a 5hr ^{51}Cr-release with purified $CD25^{lo}$ and $CD25^{hi}$ effector populations (Kaech et al., 2002). For analyzing the recall proliferation potential of donor cells, memory cells arising from $CD25^{lo}$ and $CD25^{hi}$ sorted effectors were isolated from spleens of recipient mice by column purification of CD8+ cells. For ensuring minimal contamination with endogenous cells, a second round of negative purification was performed with a Thy1.2 column.

Microarray Hybridization and Analysis

Naive, memory and day 3.5 $CD25^{lo}$ and $CD25^{hi}$ Thy1.1+ P14 CD8+ T cells were FACS sorted, and RNA was isolated, amplified, and biotinylated as described previously (Kaech et al., 2002; Sarkar et al., 2008). Samples were hybridized on mouse 430.2 Affymetrix microarray chips (Santa Clara, CA, USA) at the Vanderbilt Microarray Shared Resource (Vanderbilt University, TN, USA) in accordance with the manufacturer's protocols. Raw data were normalized with RMA package built within Genespring 7.0 (Agilent Technologies, Santa Clara, CA, USA) and fold-change comparisons between indicated groups were subsequently made. Pathway analysis was performed with the Ingenuity platform from Ingenuity Systems (Redwood City, CA, USA).

RT-PCR Analysis

Naive, memory, day 3.5 $CD25^{lo}$ and $CD25^{hi}$ and day 8.0 effector Thy1.1+ P14 CD8+ T cells were FACS sorted and RNA was isolated from cells in Trizol (GIBCO/BRL Life Technologies, Rockville, MD) according to the manufacturer's protocol. cDNA was synthesized using SuperScript Choice cDNA synthesis kit (GIBCO/BRL). Primers for RT-PCR to quantitate mRNA levels of perforin, granzyme B, T-bet, Blimp-1, CD127, CD62L and CD25 were obtained from QIAGEN (Valencia, CA) and RT-PCR performed according to their recommended protocol.

ACCESSION NUMBERS

The microarray data are available in the Gene Expression Omnibus (GEO) database (http://www.ncbi.nlm.nih.gov/gds) under the accession number GSE19825.

SUPPLEMENTAL INFORMATION

Supplemental Information includes six figures and one table and can be found with this article online at doi:10.1016/j.immuni.2009.11.010.

ACKNOWLEDGMENTS

The authors wish to acknowledge support from NIH Grant AI30048 (RA), Bill and Melinda Gates Foundation Grant CAVD 38645 (R.A.), and Elizabeth Glaser Pediatric AIDS Foundation Scholar awards (S.S. and V.K.). We wish to thank B.T. Konieczny, R. Karaffa and M. Hulsey for their excellent technical assistance.

Received: October 1, 2008
Revised: August 26, 2009
Accepted: November 3, 2009
Published online: January 21, 2010

REFERENCES

Ahmed, R., and Rouse, B.T. (2006). Immunological Memory. Immunol. Rev. *211*, 5–7.

Badovinac, V.P., and Harty, J.T. (2006). Programming, demarcating, and manipulating CD8+ T-cell memory. Immunol. Rev. *211*, 67–80.

Badovinac, V.P., Porter, B.B., and Harty, J.T. (2002). Programmed contraction of CD8(+) T cells after infection. Nat. Immunol. *3*, 619–626.

Blattman, J.N., Grayson, J.M., Wherry, E.J., Kaech, S.M., Smith, K.A., and Ahmed, R. (2003). Therapeutic use of IL-2 to enhance antiviral T-cell responses in vivo. Nat. Med. *9*, 540–547.

Calame, K. (2008). Activation-dependent induction of Blimp-1. Curr. Opin. Immunol. *20*, 259–264.

Chang, J.T., Palanivel, V.R., Kinjyo, I., Schambach, F., Intlekofer, A.M., Banerjee, A., Longworth, S.A., Vinup, K.E., Mrass, P., Oliaro, J., et al. (2007). Asymmetric T lymphocyte division in the initiation of adaptive immune responses. Science *315*, 1687–1691.

Cheng, L.E., and Greenberg, P.D. (2002). Selective delivery of augmented IL-2 receptor signals to responding CD8+ T cells increases the size of the acute antiviral response and of the resulting memory T cell pool. J. Immunol. *169*, 4990–4997.

Cheng, L.E., Ohlen, C., Nelson, B.H., and Greenberg, P.D. (2002). Enhanced signaling through the IL-2 receptor in CD8+ T cells regulated by antigen recognition results in preferential proliferation and expansion of responding CD8+ T cells rather than promotion of cell death. Proc. Natl. Acad. Sci. USA *99*, 3001–3006.

Cousens, L.P., Orange, J.S., and Biron, C.A. (1995). Endogenous IL-2 contributes to T cell expansion and IFN-gamma production during lymphocytic choriomeningitis virus infection. J. Immunol. *155*, 5690–5699.

Gillis, S., Ferm, M.M., Ou, W., and Smith, K.A. (1978). T cell growth factor: Parameters of production and a quantitative microassay for activity. J. Immunol. *120*, 2027–2032.

Gong, D., and Malek, T.R. (2007). Cytokine-dependent Blimp-1 expression in activated T cells inhibits IL-2 production. J. Immunol. *178*, 242–252.

Intlekofer, A.M., Takemoto, N., Kao, C., Banerjee, A., Schambach, F., Northrop, J.K., Shen, H., Wherry, E.J., and Reiner, S.L. (2007). Requirement for T-bet in the aberrant differentiation of unhelped memory CD8+ T cells. J. Exp. Med. *204*, 2015–2021.

Janas, M.L., Groves, P., Kienzle, N., and Kelso, A. (2005). IL-2 regulates perforin and granzyme gene expression in CD8+ T cells independently of its effects on survival and proliferation. J. Immunol. *175*, 8003–8010.

Joshi, N.S., Cui, W., Chandele, A., Lee, H.K., Urso, D.R., Hagman, J., Gapin, L., and Kaech, S.M. (2007). Inflammation directs memory precursor and short-lived effector CD8(+) T cell fates via the graded expression of T-bet transcription factor. Immunity *27*, 281–295.

Kaech, S.M., and Ahmed, R. (2001). Memory CD8+ T cell differentiation: Initial antigen encounter triggers a developmental program in naive cells. Nat. Immunol. *2*, 415–422.

Kaech, S.M., Hemby, S., Kersh, E., and Ahmed, R. (2002). Molecular and functional profiling of memory CD8+ T cell differentiation. Cell *111*, 837–851.

Kaech, S.M., Tan, J.T., Wherry, E.J., Konieczny, B.T., Surh, C.D., and Ahmed, R. (2003). Selective expression of the interleukin 7 receptor identifies effector CD8+ T cells that give rise to long-lived memory cells. Nat. Immunol. *4*, 1191–1198.

Kalia, V., Sarkar, S., Gourley, T.S., Rouse, B.T., and Ahmed, R. (2006). Differentiation of memory B and T cells. Curr. Opin. Immunol. *18*, 255–264.

Kersh, E.N., Kaech, S.M., Onami, T.M., Moran, M., Wherry, E.J., Miceli, M.C., and Ahmed, R. (2003). TCR signal transduction in antigen-specific memory CD8+ T cells. J. Immunol. *170*, 5455–5463.

Kolumam, G.A., Thomas, S., Thompson, L.J., Sprent, J., and Murali-Krishna, K. (2005). Type I interferons act directly on CD8+ T cells to allow clonal expansion and memory formation in response to viral infection. J. Exp. Med. *202*, 637–650.

Krutzik, P.O., Clutter, M.R., and Nolan, G.P. (2005a). Coordinate analysis of murine immune cell surface markers and intracellular phosphoproteins by flow cytometry. J. Immunol. *175*, 2357–2365.

Krutzik, P.O., Hale, M.B., and Nolan, G.P. (2005b). Characterization of the murine immunological signaling network with phosphospecific flow cytometry. J. Immunol. *175*, 2366–2373.

Lenardo, M.J. (1991). Interleukin-2 programs mouse alpha beta T lymphocytes for apoptosis. Nature *353*, 858–861.

Liu, C.C., Rafii, S., Granelli-Piperno, A., Trapani, J.A., and Young, J.D. (1989). Perforin and serine esterase gene expression in stimulated human T cells. Kinetics, mitogen requirements, and effects of cyclosporin A. J. Exp. Med. *170*, 2105–2118.

Malek, T.R. (2008). The biology of interleukin-2. Annu. Rev. Immunol. *26*, 453–479.

Manders, P.M., Hunter, P.J., Telaranta, A.I., Carr, J.M., Marshall, J.L., Carrasco, M., Murakami, Y., Palmowski, M.J., Cerundolo, V., Kaech, S.M., et al. (2005). BCL6b mediates the enhanced magnitude of the secondary response of memory CD8+ T lymphocytes. Proc. Natl. Acad. Sci. USA *102*, 7418–7425.

Martins, G., and Calame, K. (2008). Regulation and functions of Blimp-1 in T and B lymphocytes. Annu. Rev. Immunol. *26*, 133–169.

Martins, G.A., Cimmino, L., Liao, J., Magnusdottir, E., and Calame, K. (2008). Blimp-1 directly represses Il2 and the Il2 activator Fos, attenuating T cell proliferation and survival. J. Exp. Med. *205*, 1959–1965.

Marzo, A.L., Klonowski, K.D., Le Bon, A., Borrow, P., Tough, D.F., and Lefrancois, L. (2005). Initial T cell frequency dictates memory CD8+ T cell lineage commitment. Nat. Immunol. *6*, 793–799.

Mercado, R., Vijh, S., Allen, S.E., Kerksiek, K., Pilip, I.M., and Pamer, E.G. (2000). Early programming of T cell populations responding to bacterial infection. J. Immunol. *165*, 6833–6839.

Murali-Krishna, K., Altman, J.D., Suresh, M., Sourdive, D.J., Zajac, A.J., Miller, J.D., Slansky, J., and Ahmed, R. (1998). Counting antigen-specific CD8+ T cells: A reevaluation of bystander activation during viral infection. Immunity *8*, 177–187.

Pandiyan, P., Zheng, L., Ishihara, S., Reed, J., and Lenardo, M.J. (2007). CD4+CD25+Foxp3+ regulatory T cells induce cytokine deprivation-mediated apoptosis of effector CD4+ T cells. Nat. Immunol. *8*, 1353–1362.

Pipkin, M.E., Sacks, J.A., Cruz-Guilloty, F., Lichtenheld, M.G., Bevan, M.J., and Rao, A. (2010). Interleukin-2 and inflammation induce distinct transcriptional programs that promote the differentiation of effector cytolytic T cells. Immunity *32*, this issue, 79–90.

Pulendran, B., and Ahmed, R. (2006). Translating innate immunity into immunological memory: Implications for vaccine development. Cell *124*, 849–863.

Rutishauser, R.L., Martins, G.A., Kalachikov, S., Chandele, A., Parish, I.A., Meffre, E., Jacob, J., Calame, K., and Kaech, S.M. (2009). Transcriptional repressor Blimp-1 promotes CD8+ T cell terminal differentiation and represses the acquisition of central memory T cell properties. Immunity *31*, 178–180.

Sadlack, B., Merz, H., Schorle, H., Schimpl, A., Feller, A.C., and Horak, I. (1993). Ulcerative colitis-like disease in mice with a disrupted interleukin-2 gene. Cell *75*, 253–261.

Sarkar, S., Kalia, V., Haining, W.N., Konieczny, B.T., Subramaniam, S., and Ahmed, R. (2008). Functional and genomic profiling of effector CD8+ T cell subsets with distinct memory fates. J. Exp. Med. *205*, 625–640.

Smith, K.A. (1988). Interleukin-2: Inception, impact, and implications. Science *240*, 1169–1176.

Smith, K.A., and Cantrell, D.A. (1985). Interleukin 2 regulates its own receptors. Proc. Natl. Acad. Sci. USA *82*, 864–868.

Suzuki, H., Kundig, T.M., Furlonger, C., Wakeham, A., Timms, E., Matsuyama, T., Schmits, R., Simard, J.J., Ohashi, P.S., Griesser, H., et al. (1995). Deregulated T cell activation and autoimmunity in mice lacking interleukin-2 receptor beta. Science *268*, 1472–1476.

van Stipdonk, M.J., Lemmens, E.E., and Schoenberger, S.P. (2001). Naive CTLs require a single brief period of antigenic stimulation for clonal expansion and differentiation. Nat. Immunol. *2*, 423–429.

van Stipdonk, M.J., Hardenberg, G., Bijker, M.S., Lemmens, E.E., Droin, N.M., Green, D.R., and Schoenberger, S.P. (2003). Dynamic programming of CD8+ T lymphocyte responses. Nat. Immunol. *4*, 361–365.

Wherry, E.J., Teichgraber, V., Becker, T.C., Masopust, D., Kaech, S.M., Antia, R., von Andrian, U.H., and Ahmed, R. (2003). Lineage relationship and protective immunity of memory CD8+ T cell subsets. Nat. Immunol. *4*, 225–234.

Williams, M.A., and Bevan, M.J. (2007). Effector and memory CTL differentiation. Annu. Rev. Immunol. *25*, 171–192.

Williams, M.A., Tyznik, A.J., and Bevan, M.J. (2006). Interleukin-2 signals during priming are required for secondary expansion of CD8+ memory T cells. Nature *441*, 890–893.